

## Ameliorative effects of the ethanolic extract of *Allium saralicum* R.M. Fritsch on CCl<sub>4</sub>-induced nephrotoxicity in mice: A stereological examination

Hamidreza Sherkatolabbasieh<sup>1</sup>, Lida Hagh-Nazari<sup>2</sup>, Shiva Shafieezadeh<sup>3</sup>, Nader Goodarzi<sup>4\*</sup>, Mohammad Mehdi Zangeneh<sup>2,5</sup> and Akram Zangeneh<sup>2,5</sup>

<sup>1</sup> Department of Pediatrics, School of Medicine, Lorestan University of Medical Sciences, Khoramabad, Iran

<sup>2</sup> Department of Biochemistry, Faculty of Medicine, Kermanshah University of Medical Science, Kermanshah, Iran

<sup>3</sup> Department of Internal Medicine, Lorestan University of Medical Sciences, Khoramabad, Iran

<sup>4</sup> Department of Basic Science, Faculty of Veterinary Medicine, Razi University, Kermanshah, Iran

<sup>2,5</sup> Faculty of Veterinary Medicine, Razi University, Kermanshah, Iran

\*Corresponding author: n.goodarzi@razi.ac.ir

Received: September 14, 2016; Revised: November 18, 2016; Accepted: November 21, 2016; Published online: November 28, 2016

**Abstract:** The present study was carried out to investigate the nephroprotective effect of the ethanolic extract of *Allium saralicum* R.M. Fritsch (ASRMF) in mice. Thirty-five male mice were divided into five groups (n=7). Group 1 (positive control) received 1 mL/kg olive oil intraperitoneally (i.p.) and 0.5 mL distilled water orally; Group 2 (negative control) received CCl<sub>4</sub> (50% in olive oil, 1 mg/kg; i.p.); Groups 3, 4 and 5 received CCl<sub>4</sub> and 200, 800 and 1600 µg/kg of ASRMF extract, respectively. The renal volume and cortex in Groups 1 and 2 were increased by 55% and 62% ( $p \leq 0.001$ ) following CCl<sub>4</sub> administration, respectively, and were improved after ASRMF administration. The volume of proximal convoluted tubules (PCTs), glomeruli, vessels and interstitial tissue increased 80%, 150%, 83% and 64% ( $p \leq 0.05$ ), respectively, in CCl<sub>4</sub>-treated mice, and decreased significantly with 800 and 1600 µg/kg of ASRMF. The length of PCTs and vessels increased 51% and 45% and decreased ( $p \leq 0.05$ ) with 200, 800 and 1600 µg/kg of ASRMF, respectively. CCl<sub>4</sub>-treated mice lost 22.5% of glomeruli; the loss was inhibited significantly ( $p \leq 0.05$ ) by ASRMF. Urea and creatinine concentrations were increased ( $p \leq 0.05$ ) in CCl<sub>4</sub>-induced nephrotoxicity as compared to the controls, whereas different doses of ASRMF restored the levels of these biomarkers compared to the negative controls. In conclusion, ASRMF has a potent nephroprotective property and can improve renal structural and serum biomarkers in CCl<sub>4</sub>-induced nephrotoxicity in mice.

**Key words:** carbon tetrachloride; *Allium saralicum*; kidney; nephrotoxicity; stereology

### INTRODUCTION

Carbon tetrachloride (CCl<sub>4</sub>), a clear, colorless, volatile, heavy and nonflammable liquid is a potent environmental hepatotoxin and nephrotoxin that causes steatosis, necrosis and cirrhosis [1]. CCl<sub>4</sub> intoxication causes free radical generation in many tissues, such as the liver, kidneys, heart, lung, testes, brain and blood [2-5]. The initial step in the tissue injury induced by CCl<sub>4</sub> is the cytochrome P450-mediated transfer of a single electron to the C-Cl bond, which gives rise to a radical anion as a transient intermediate that eliminates chlorine to form a carbon-centered radical, the trichloromethyl radical ·CCl<sub>3</sub>, and chloride [6,7]. The ·CCl<sub>3</sub> in the presence of oxygen is subsequently converted into an even more reactive trichloromethyl

peroxyl radical (·OOCCL<sub>3</sub>) that initiates the process of lipid peroxidation [8] and production of membrane-damaging products such as malondialdehyde (MDA). It is believed that the free radical-induced lipid peroxidation is one of the major causes of cell membrane damage that leads to a number of pathological states causing acute and chronic renal injuries [9-11]. Furthermore, various documented case studies have established that CCl<sub>4</sub> produces renal disease with an altered antioxidant status in humans [12,10].

Findings from the screening of different medicinal plants describe their antioxidant properties and indicate that they could protect organs against CCl<sub>4</sub>-induced oxidative stress by altering the levels of antioxidant enzymes [13,14].

*Allium saralicum* (Valak Soori in Persian) is an endemic plant of Iran that grows widely in the western parts of the country. The genus *Allium* is placed in the family *Amaryllidaceae* and subfamily *Allioideae*. The cooking and consumption of parts of the plant is due to the large variety of flavors and textures of the species. Various *Allium* species have been cultivated from the earliest times and about a dozen species are economically important as crops or garden vegetables, and some species are important as ornamental plants [15,16].

In the present study, we investigated the ameliorative effect of the ethanolic extract of *Allium saralicum* by studying the microscopic structural changes in mice kidney after  $\text{CCl}_4$ -induced nephrotoxicity using modern design-based stereological methods. The stereological variables are volume of the renal cortex, medulla, glomeruli, connective tissues, proximal and distal convoluted tubules, vessels, collecting ducts, Henle's loop and lengths of the five last-mentioned tubular structures. Renal functions were also investigated by examining serum biomarkers, urea and creatinine.

## MATERIALS AND METHODS

### Plant collection

Mature *Allium saralicum* plants were collected from around Kermanshah city during April 2015. The plant was identified for the first time and a voucher specimen (no. 2738RUH) was deposited at the herbarium of the Research Center of the Faculty of Agriculture, Razi University, Kermanshah, Iran.

### Plant extraction

All parts of the plant (leaves, stem, flowers, seeds and roots) were shade-dried for one week. The dried aerial parts of the plants were ground and about 150 g of the obtained powder was extracted with 450 mL of 100% ethanol for 2 h at 40°C with continuous shaking. The extract was left for 24 h at room temperature and then filtered through Whatman filter paper #2. The obtained extract was concentrated under reduced pressure using a rotary evaporator (Panchun Scientific Co., Kaohsiung, Taiwan) at 80°C until a semi-solid sticky mass was obtained. Since all ethanol evaporates completely during

**Table 1.** The components of *Allium saralicum* R.M. Fritsch analyzed by GC/MS.

No	Compound	Area (%)
1	Neophytadiene	11.6
2	2-Hexadecene, 3,7,11,15-tetramethyl	1.4
3	Hexadecanoic acid	6.4
4	Phytol	14.1
5	Linolenic acid, methyl ester	24.4
6	Hexanedioic acid, bis(2-ethylhexyl) ester	1.2
7	1,4,8,11-Tetraazacyclotetradecane	1.2
8	Hexatriacontane	3.3
9	Nonadecene	5.6
10	Ethanol, 2-tetradecyloxy	6
11	$\gamma$ -Tocopherol	3
12	Eicosane	2.9
13	Vitamin E	6.1
14	2-Phenyl-5-methylindole	6.8
15	N-ethyl-1,3-dithioisindoline	2.1

the extraction process, the extract does not induce any ethanol-related adverse effects following administration. The components of this extract were analyzed by gas chromatography/mass spectrometry (GC/MS) in the Research Center of Razi University. The complete details of this GC/MS are presented in Table 1.

### Animals and treatments

Thirty-five healthy male BALB/c mice weighing between 35 and 40 g were obtained from the laboratory animal center of Kermanshah University of Medical Sciences. The animals were kept under constant humidity and temperature. All animals were allowed access to food and water *ad libitum* during the experiment. The animals were treated according to the standard directive, as recommended in the Guide for Care and Use of Laboratory Animals [17] approved by the research authorities of Kermanshah University of Medical Sciences. The mice were divided randomly into five groups ( $n=7$ ) as follows: Group I (control) received 1 mL/kg olive oil i.p. and 0.5 mL distilled water by gavage; Group II received 1 mg/kg  $\text{CCl}_4$  mixed with olive oil at a ratio of 5:5 i.p., and 0.5 mL distilled water by gavage; Group III received  $\text{CCl}_4$  mixed with olive oil at a ratio of 5:5 i.p. and *Allium saralicum* R.M. Fritsch (ASRMF) (200  $\mu\text{g}/\text{kg}$  bw) by gavage; Group IV received  $\text{CCl}_4$  mixed with olive oil at a ratio of 5:5 i.p. and ASRMF (800  $\mu\text{g}/\text{kg}$  bw) by gavage; Group V received  $\text{CCl}_4$  mixed with olive oil

at a ratio of 5:5 i.p. and *ASRMF* (1600 µg/kg bw) by gavage. All administrations were performed twice a week (on Saturday and Wednesday) for 45 days. After completion of the experiment, the animals were weighed and killed by chloroform inhalation. Blood samples were obtained from the animals' heart tubes that were centrifuged to obtain the serum. The left kidney of each animal was removed and cleaned of perirenal fat and connective tissue. The kidney was then weighed and the primary volume was measured using the immersion method [18]. The kidney was fixed in neutral buffered formaldehyde for 5 days. To prevent reference trap, the reference volume or the final volume of the kidney must be estimated [19,20]. The reference volume was estimated by calculating shrinkage after tissue processing and staining without any need for serial sections. Estimation of shrinkage and tubule length requires isotropic uniform random sections [19,21]. These sections were obtained by the orientator method. Briefly, each kidney was placed on a circle on which each half was divided into 10 equal distances ( $\phi$ -clock), a random number between 0 and 10 was selected and the kidney was sectioned into two halves with a blade in this direction. The cut surface of one half of the kidney was then placed along the 0-0 direction of the second circle with 10 unequal sinus-weighted divisions ( $\theta$ -clock) and the second cut was done by selecting a random number. The cut surface of the other half of the kidney was placed vertically on the  $\theta$ -clock. The second cut was done by selecting a random number. The entire kidney was sectioned with a blade, placed in the direction of the second cuts with an interval of 1 mm. The slabs (7-10 slabs) were then collected. A circle was punched from a kidney slab by a trocar. The diameters of the circular piece of the kidney were measured by a micrometer and the area of the circle was estimated using the usual formula for calculating the area of a circle. The slabs and circular pieces were embedded in paraffin and 5 µm-thick sections were prepared and stained by the Periodic Acid Schiff (PAS) method. After staining, the area of the circular piece was measured again and the volume shrinkage was calculated as:

$$\text{Volume shrinkage} = 1 - \left(\frac{AA}{AB}\right)^{1.5}$$

where AA and AB are the areas of the circular piece after and before tissue processing, respectively. Af-

ter estimating the shrinkage, the final volume of the kidney (the reference space) was corrected using the following formula:

$$V_{\text{final}} = V_{\text{primary}} \times (1 - \text{volume shrinkage})$$

### Stereological study: volume estimation

Each sampled section was analyzed using a video-microscopy system equipped with a microscope (Olympus CX2, Japan) linked to a video camera (Dinocapture ver. 5; dino-lit.com; 30.5 mm), a P4 PC computer and a monitor to determine the parameters. Between 10 and 14 microscopic fields were examined in each kidney. The point probe (composed of 20 points) was superimposed on the images of the tissue sections viewed on the monitor and volume densities ( $V_v$ ) of the renal cortex, medulla, glomeruli, proximal convoluted tubule (PCT), distal convoluted tubule (DCT), collecting ducts (CD), loop of Henle (LH), vessels and connective tissue were obtained using a point-counting method (Fig. 1) and the following formula [19]:

$$V_v = \frac{P_{\text{structure}}}{P_{\text{reference}}}$$

where  $P_{\text{structure}}$  and  $P_{\text{reference}}$  are the number of test points falling on the structure's profile and on the reference space, respectively. One section and 10-14 microscopic fields were examined in each kidney. The absolute volume of the parameters was estimated by

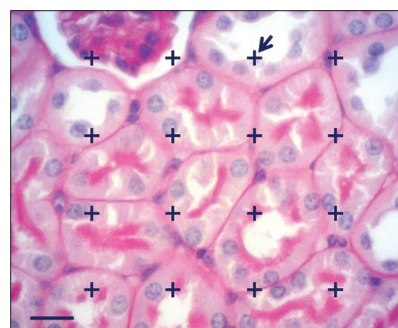


**Fig. 1.** Microscopic section of the kidney showing the glomerulus, proximal and distal convoluted tubules. To estimate volume density, the total number of points hitting each component (the point is the right upper corner of the cross, the arrow) was divided by the total number of points hitting the reference space. Scale bar 50 µm PAS, 400×.

multiplying the fractional volume by the final volume of the kidney to prevent the reference trap [21,22].

### Length estimation

The length densities of the renal tubules and vessels were estimated by randomly superimposing an unbiased counting frame (740×740 μm) on the monitor live images. The tubule profiles completely inside the counting frame or partly inside the counting frame but only touching the top and right lines were counted. The tubule profiles touching the bottom and left lines and its extensions were ignored (Fig. 2). The length density ( $L_v$ ) of the each tubule was calculated as:

$$L_v = 2 \times \frac{\Sigma Q}{a(\text{frame}) \times \Sigma \text{ frame}}$$

where  $\Sigma Q$  denotes the total number of the tubule profiles counted per mouse kidney;  $a(\text{frame})$  equals the area associated with a frame, 547600 μm<sup>2</sup> and  $\Sigma \text{ frame}$  is the total number of frames counted. The total length of each tubule in mouse kidney ( $L$ ) was calculated by multiplying the length density ( $L_v$ ) by the final volume of the kidney [19,21].

### Number estimation

The total number of glomeruli per kidney was estimated by the physical dissector method [23]. From each kidney, a section pair 20 μm apart (the 1<sup>st</sup> and 5<sup>th</sup> sections) was obtained. Two separate projecting systems with similar equipment were used. Two dissector probes (740×740 μm) with exclusion lines (the left and lower borders) and inclusion lines (the right and upper borders) were superimposed on the images of the 1<sup>st</sup> section, which served as the reference section (Fig. 3a), and the 7<sup>th</sup> section as the look-up section (Fig. 3b) at 135× magnification. A glomerulus was counted if it was presented in a reference section but not in the look-up section and if it did not touch the exclusion lines. At least 100 glomeruli per kidney were counted. The numerical density of the glomeruli was estimated using:

$$N_v = \frac{\Sigma Q^-}{a(\text{frame}) \times h \times \Sigma P}$$

where  $\Sigma Q^-$  denotes the number of counted glomeruli,  $a(\text{frame})$  is the area of the dissector frame,  $\Sigma P$  is the

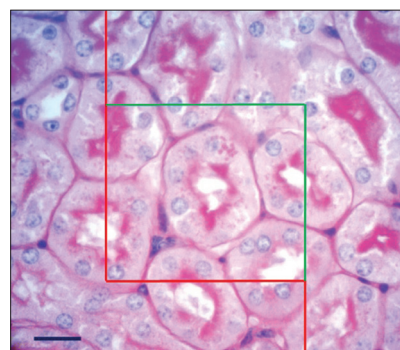


**Fig. 2.** The length density of the renal tubules is estimated by an unbiased counting frame on the images. The tubule profiles completely inside the counting frame or partly inside the counting frame but only touching the top and right lines are counted (here 5 proximal convoluted tubules). The tubule profiles touching the bottom and left lines and its extensions are ignored. Scale bar 50 μm, PAS, 400×.

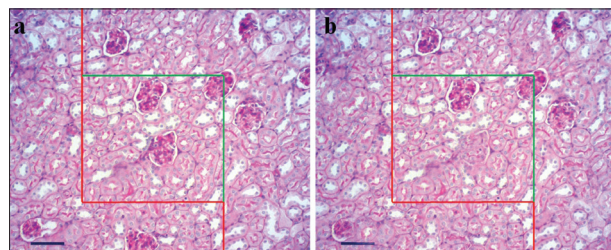


**Fig. 3.** For estimating the numerical density of glomeruli according to the physical dissector method, the images of two sections 20 μm apart (1<sup>st</sup> and 5<sup>th</sup> sections) were used as (a) a reference and (b) the look-up section, respectively. An unbiased counting frame is superimposed on the sample sections. Glomerular profiles are counted if they are contained completely or partly in the frame and are not hit by exclusion (red lines), and if they disappeared in the look-up section (here 1). Scale bars 100 μm, PAS, 100×.

sum of studied field and  $h$  is the dissector height. The total glomerular number was estimated by multiplying the numerical density ( $N_v$ ) by the reference volume (renal cortex).

### Biochemical analysis

The serum biomarkers, urea and creatinine, were measured by a spectrophotometric procedure and determined as markers of kidney function using kits (Ziest Chem Diagnostics) according to the manufacturers' instructions. All biochemical measures were done in duplicate.

## Statistical analysis

The data are expressed as the means±standard deviation. A statistical comparison between group means was performed by one-way ANOVA followed by Tukey's post-hoc test.  $P \leq 0.05$  was considered as significant.

**Table 2.** Kidney weight (mg), absolute volume of the kidney ( $\text{mm}^3$ ), and absolute volumes ( $\text{mm}^3$ ) of the cortex and medulla of the control and experimental groups treated with *Allium saralicum* R.M. Fritsch. Results are given as means±standard deviation.

Groups (n=7)	Parameters			
	Kidney weight (mg)	Kidney volume ( $\text{mm}^3$ )	Cortex volume ( $\text{mm}^3$ )	Medulla volume ( $\text{mm}^3$ )
Control	135.2±1.4	110.5±2.9	77.77±4.3	25.3±3.2
CCl <sub>4</sub>	195±15.6*	171±14.7*	125±11.8 *	30.9±13.7
T200	189±35*	163.2±10.2 *	121.8±10.3 *	28.2±5.1
T800	168±14.7**	140.7±7.1**	105±8**	28.9±6
T1600	160±46**	128.5±10.1**	92±14**	26.3±5.8

\*  $p \leq 0.05$  vs the control group

\*\*  $p \leq 0.05$  vs the CCl<sub>4</sub>-treated group

**Table 3.** Absolute volume ( $\text{mm}^3$ ) of the proximal and distal convoluted tubules (PCT, DCT), collecting ducts (CD), loop of Henle (LH), vessels (VES) and interstitial tissues (IT) in the control and experimental groups treated with *Allium saralicum* R.M. Fritsch. Results are given as means±standard deviation.

Groups (n=7)	Parameters					
	PCT ( $\text{mm}^3$ )	DCT ( $\text{mm}^3$ )	CD ( $\text{mm}^3$ )	LH ( $\text{mm}^3$ )	VES ( $\text{mm}^3$ )	IT ( $\text{mm}^3$ )
C	68.5±4	16.5±3	20.9±4	1.20±0.4	6.1±1.2	11.4±2
CCl <sub>4</sub>	122.2±12*	22.5±5.7	25.4±5.1	1.36±0.65	11.2±4.2*	18.7±4.5*
T200	96.8±7.4	22.5±3.4	23.8±5.7	1.30±0.41	9.4±2.2	15.2±5
T800	84.4±7.2**	18.6±4.6	22.1±5.2	1.31±0.36	6.9±1.7**	14±2.7**
T1600	78.1±15**	15.2±4	22.9±6.4	1.25±0.28	6.5±2.5**	11.6±4**

\*  $p \leq 0.05$  vs the control group

\*\*  $p \leq 0.05$  vs the CCl<sub>4</sub>-treated group

**Table 4.** Absolute volume ( $\text{mm}^3$ ) and number of the glomeruli (GLOM) in the control and experimental groups treated with *Allium saralicum* R.M. Fritsch. Results are given as means±standard deviation.

Groups (n=7)	Parameters	
	Volume ( $\text{mm}^3$ )	Number
C	0.002±0.0001	28990.4±1851.5
CCl <sub>4</sub>	0.005±0.0003*	22474.8±856.3*
T200	0.004±0.0002	22881.9±1385.7
T800	0.004±0.0002	26722±1222.4**
T1600	0.002±0.0003**	27010±965.7**

\*  $p \leq 0.05$  vs the control group

\*\*  $p \leq 0.05$  vs the CCl<sub>4</sub>-treated group

## RESULTS

### Effects of CCl<sub>4</sub> and ASRMF on the weight and volumes of the kidney and of its components

The data regarding kidney weight, mean absolute volume of kidney and its components in control and treated groups are presented in Tables 2-4. The kidney weight and volume were increased by 44% and 55% ( $p \leq 0.001$ ), respectively, in CCl<sub>4</sub>-treated mice in comparison with the control group. The volume of the cortex increased 62% ( $p \leq 0.001$ ) in this group, but the medulla only increased 22%, which was not significant ( $p > 0.05$ ) in comparison with the control group. Treatment of CCl<sub>4</sub>-treated mice with 800 and 1600  $\mu\text{g}/\text{kg}$  of ASRMF significantly ( $p \leq 0.05$ ) improved kidney weight and kidney volume. Further, the volume of the cortex was decreased significantly ( $p \leq 0.05$ ) in both ASRMF-treated groups as compared to the CCl<sub>4</sub>-treated group, whereas, the medulla volume did not exhibit a significant decrease ( $p > 0.05$ ).

The volumes of PCT, GLOM, vessels and interstitial tissue were increased 80%, 150%, 83% and 64% ( $p \leq 0.05$ ), respectively, in the CCl<sub>4</sub>-treated mice as compared to the controls (Tables 3 and 4). The volumes of the collecting duct (CD) and loop of Henle (LH) did not show significant differences ( $p > 0.05$ ). Treatment of mice with 800 and 1600  $\mu\text{g}/\text{kg}$  of ASRMF significantly ( $p \leq 0.05$ ) decreased the volume of PCTs, vessels and interstitial tissue as compared to the CCl<sub>4</sub>-treated group, while the glomerular volume was decreased significantly ( $p \leq 0.05$ ) after treatment with the highest dose of ASRMF in comparison to the CCl<sub>4</sub>-treated mice.

### Effects of CCl<sub>4</sub> and ASRMF on renal tubule and vessel lengths

The length of the PCT and vessels increased 51% and 45%, respectively ( $p \leq 0.05$ ), following CCl<sub>4</sub> administration. ASRMF (800 and 1600  $\mu\text{g}/\text{kg}$ ) shifted these values toward the control values (Table 5). The increases in length of DCT, CD and LH were not significant ( $p > 0.05$ ) in the CCl<sub>4</sub>-treated mice as compared to the control.

### Effects of CCl<sub>4</sub> and ASRMF on glomerular number

The obtained results showed that the number of glomeruli per kidney in the CCl<sub>4</sub>-treated group were significantly (22.5%) lower than in control animals. Coadministration of either 800 or 1600 µg/kg ASRMF and CCl<sub>4</sub> significantly inhibited the decrease in the number of glomeruli ( $p \leq 0.05$ ) in comparison with the CCl<sub>4</sub>-treated group. The glomerular number did not significantly differ between 800 and 1600 µg/kg ASRMF (Table 4).

### Effects of CCl<sub>4</sub> and ASRMF on the serum biochemical profile

The serum concentrations of creatinine and urea serve as indicators of kidney injury and dysfunction. The effect of CCl<sub>4</sub> administration on changes in these biochemical markers are presented in Table 6. The concentrations of urea and creatinine were increased in the serum in CCl<sub>4</sub>-induced nephrotoxicity as compared to the control group. However, the increase in urea was not significant ( $p > 0.05$ ). Coadministration

of both CCl<sub>4</sub> and different doses of ASRMF significantly reversed the levels of these markers, pointing to recovery and normalization.

### DISCUSSION

The present *in vivo* study demonstrated the nephroprotective potential of the ethanol extract of *Allium saralicum* R.M. Fritsch on CCl<sub>4</sub>-induced nephrotoxicity by stereological methods. Numerous experimental studies showed that CCl<sub>4</sub> causes tissue damage in many organs, albeit mainly in the liver, and changes in several blood biochemical parameters [1,24-26]. It has been reported that CCl<sub>4</sub> systemically administered to rats is distributed at higher concentrations in the kidney than in the liver [27,28]. Since the kidney has an affinity for CCl<sub>4</sub> and contains cytochrome P450 predominantly in the cortex [1,29,30], CCl<sub>4</sub> is likely to contribute to nephrotoxicity.

In this study, after exposure of experimental animals to 1 mg/kg bw of CCl<sub>4</sub>, we observed a significant increase in serum biomarkers, creatinine and urea, which is in agreement with previous reports [26,31,32]. The increase in serum urea and creatinine was inhibited significantly in groups that received simultaneously 800 and 1600 µg/kg body weight of ASRMF and CCl<sub>4</sub> in comparison with CCl<sub>4</sub>-treated mice. Similar investigations have also documented that different plant extracts significantly recovered biochemical marker fluctuations induced by CCl<sub>4</sub> intoxication [5,31]. Such effects might be related to the antioxidant properties of these plant extracts. Based on the results of GC/MS analysis, linolenic acid constitutes the main part of the ethanolic extract of ASRMF. Recent research has shown that oral intake of  $\alpha$ -linolenic acid is beneficial in experimental colitis, myocardial infarction, arterial thrombus formation and osteoporosis. There is also evidence of the protective role of plant  $\Omega$ 3 against nephrotoxicity induced by gentamicin [32]. Based on previous investigations,  $\alpha$ -linolenic acid has antioxidant and anti-inflammatory activities. This fatty acid has a strong inhibitory effect on the production of NO and iNOS and TNF- $\alpha$  gene expression by blocking NF- $\kappa$ B and MAPK activation. The ability of  $\alpha$ -linolenic acid to regulate the expression of NF- $\kappa$ B, TNF- $\alpha$  and inflammatory interleukins may account for its protective effects [33].

**Table 5.** Absolute length (m) of the proximal and distal convoluted tubules (PCT, DCT), collecting ducts (CD), loop of Henle (LH) and vessels (VES) in the control and experimental groups treated with *Allium saralicum* R.M. Fritsch. Results are given as means  $\pm$  standard deviation.

Groups (n=7)	Parameters				
	PCT (m)	DCT (m)	CD (m)	LH (m)	VES (m)
C	33.8 $\pm$ 5.7	23 $\pm$ 3.3	42.3 $\pm$ 5.7	19.5 $\pm$ 4.4	56.6 $\pm$ 11.7
CCl <sub>4</sub>	51.2 $\pm$ 9.1*	32 $\pm$ 5.4	51.1 $\pm$ 6.6	22.3 $\pm$ 4.3	82 $\pm$ 13.3*
T200	46.4 $\pm$ 5.8	30.1 $\pm$ 4.7	55.8 $\pm$ 7.4	20.1 $\pm$ 5	75.1 $\pm$ 9.5
T800	40.4 $\pm$ 7.8	27.1 $\pm$ 5.1	57 $\pm$ 13.5	22.6 $\pm$ 5.6	63.9 $\pm$ 12.3**
T1600	35.6 $\pm$ 6.3**	28 $\pm$ 7.2	48 $\pm$ 9.2	18.6 $\pm$ 4.3	57.5 $\pm$ 12.7**

\*  $p \leq 0.05$  vs the control group

\*\*  $p \leq 0.05$  vs the CCl<sub>4</sub>-treated group

**Table 6.** Serum profile parameters in the control and experimental groups treated with *Allium saralicum* R.M. Fritsch. Results are given as means  $\pm$  standard deviation.

Groups (n=7)	Parameters	
	Urea (mg/dl)	Creatinine (mg/dl)
C	40 $\pm$ 3.4	0.26 $\pm$ 0.05
CCl <sub>4</sub>	43.25 $\pm$ 3.77	0.37 $\pm$ 0.05*
T200	37.33 $\pm$ 6	0.26 $\pm$ 0.05**
T800	35.5 $\pm$ 6.3**	0.25 $\pm$ 0.07**
T1600	34.8 $\pm$ 6.4**	0.24 $\pm$ 0.05**

\*  $p \leq 0.05$  vs the control group

\*\*  $p \leq 0.05$  vs the CCl<sub>4</sub>-treated group

Furthermore, other compounds of *Allium saralicum*, such as phytol, neophytadiene and vitamin E, are potent antioxidant and anti-inflammatory agents [34].

As our results show, CCl<sub>4</sub>-treated animals exhibited a significant increase in kidney weight and volume. The main effect was seen on the cortex. It is well known that the renal cortex is composed mainly of the PCT and DCT. However, only the PCT was affected by CCl<sub>4</sub> as its volume and length were significantly increased. Accordingly, it was revealed that reversible alterations occur in the renal proximal tubular epithelium following CCl<sub>4</sub> administration, which is manifested by loss of basilar interdigitations, cellular swelling and swollen microvilli [36]. On the other hand, administration of CCl<sub>4</sub> resulted in an insignificant increase in the volumes of vessels and connective tissue. Oxidative stress induced by CCl<sub>4</sub> can promote the formation of a variety of vasoactive mediators that can affect renal function directly by initiating renal vasoconstriction [5]. These events may explain the increase in kidney weight and volume observed in this study. In addition to the PCT, vessels and interstitial tissue, CCl<sub>4</sub> also causes hypertrophy of glomeruli, which could be due to vasoconstriction and congestion of capillary tufts in the renal corpuscles.

Our study, with its design based on unbiased stereological methods, showed that the administration of CCl<sub>4</sub> to animals treated with *ASRMF* significantly inhibited glomerular hypertrophy and loss of glomerular number in comparison with untreated animals. There are reports that plant extracts of *Oxalis corniculata* [37], *Citharexylum spinosum* [38] and *Sonchus asper* [39] can inhibit glomerular hypertrophy in CCl<sub>4</sub>-induced nephrotoxicity.

Although the glomerular number was reduced significantly in CCl<sub>4</sub>-treated animals, there was no significant difference between the control group and mice that received 800 and 1600 µg/kg of *ASRMF*. In fact, glomerular number loss is irreversible. Because the nephrons develop during embryonic development and as there is no nephrogenesis after birth, the maintenance of glomerular number in CCl<sub>4</sub>-induced nephrotoxicity is an important potent nephroprotective effect of *ASRMF*.

The results of the present study were obtained using stereological techniques. Several methods pro-

vide potentially less variable and more sensitive and quantifiable measures of tissue changes that could be associated with biomarker appearance [40]. It should be noted that biomarkers found in biological fluids are typical indicators of functional change or cellular injury. High fidelity scanning can convert glass slides to digital images, allowing software-based, image analysis [41,42] and quantification of the injury or association with a stainable tissue protein. Software applications for stereology evaluation of digital images enhance the ability to detect and quantify changes in tissue morphology [21,43]. These methods offer potentially more sensitive methods for evaluating early and/or very mild changes in tissue morphology that might be relevant for early biomarker release and unperceivable to a trained pathologist working with light microscopy.

Finally, it can be concluded that the high dose of *ASRMF* extract has a nephroprotective effect against renal structural changes induced by CCl<sub>4</sub> in mice. This beneficial effect could be attributed to the antioxidant activities of compounds contained in the extract, such as linolenic acid, phytol, neophytadiene and vitamin E.

**Acknowledgments:** The authors would like to thank the Kermanshah University of Medical Science for the financial support. The technical assistance of Mr. Moradi and Dr. Massomi are highly appreciated.

**Authors' contribution:** HS and SS prepared the manuscript. LH performed the biochemical analysis. NG designed and performed the stereological plan. MMZ contributed in the statistical analysis. AZ was involved in animal handling and treatments. MZ prepared the plant extract.

**Conflict of interest disclosure:** The authors declare that there is no conflict of interest.

## REFERENCES

1. Abraham P, Wilfred G, Cathrine SP. Oxidative damage to the lipids and proteins of the lungs, testis and kidney of rats during carbon tetrachloride intoxication. *Clin Chim Acta*. 1999;289:177-9.
2. Rechnagel RO, Glende EA, Dolak JA, Waller RL. Mechanisms of carbon tetrachloride toxicity. *J Pharmacol Exp Ther*. 1989;43:139-54.
3. Kumar G, Banu GS, Pandian MR. Evaluation of the antioxidant activity of *Trianthemaportula castrum* L. *Ind J Pharmacol*. 2005;37:331-3.

4. Khan MR, Ahmed D. Protective effects of *Digeramuricata* (L.) Mart. on testis against oxidative stress of carbon tetrachloride in rat. *Food Chem Toxicol.* 2009;47:1393-99.
5. Khan MR, Rizvi W, Khan GN, Khan RA, Shaheen S. Carbon tetrachloride induced nephrotoxicity in rat: protective role of *Diger amuricata*. *J Ethnopharmacol.* 2009;122:91-9.
6. Slater TF. Free radical mechanisms in tissue injury. *Biochem J.* 1984;222:1-15.
7. Halliwell B, Gutteridge J. Oxygen toxicity, oxygen radicals, transition metals and disease. *Biochem J.* 1984;219:1-14.
8. Halliwell B, Gutteridge JMC. Cellular responses to oxidative stress: adaptation, damage, repair, senescence and death. In: Halliwell B, Gutteridge JMC, editors. *Free Radicals in Biology and Medicine*. Oxford: Oxford University Press Inc; 2007. 187-267 p.
9. Satyanarayana. PS, Singh D, Chopra K. Quercetin, a biflavonoid, protects against oxidative stress-related renal dysfunction by cyclosporine in rats. *Methods Find Exp Clin Pharmacol.* 2001;23:175-81.
10. Manna P, Mahua S, Parames CS. Aqueous extract of *Terminalia arjuna* prevents carbon tetrachloride-induced hepatic and renal disorders. *BMC Complement Altern Med.* 2006;6:33.
11. Adewole SO, Salako AA, Doherty OW, Naicker T. Effect of melatonin on carbon tetrachloride-induced kidney injury in Wistar rats. *Afr J Biomed Res.* 2007;10:153-64.
12. Perez AJ, Courel M, Sobrado J, Gonzalez L. Acute renal failure by tropical application of carbon tetrachloride. *Lancet.* 1987;1:515-6.
13. Ko KM, Ip SP, Poon MK, Wu SS, Che CT, Ng KH, Kong YC. Effect of a lignan-enriched *Fructus schisandrae* extract on hepatic glutathione status in rats: protection against carbon tetrachloride toxicity. *Planta Medica.* 1995;61:134-7.
14. Rajesh MG, Latha M.S. Protective activity of *Glycyrrhizalabra* Linn. on carbon tetrachloride-induced peroxidative damage. *Indian J Pharmacol.* 2004;36:284-7.
15. Block E. *Garlic and Other Alliums: The Lore and the Science*. Cambridge: Royal Society of Chemistry; 2010. 121 p.
16. Davies D. *Alliums: The Ornamental Onions*. Portland: Timber Press; 1992. 58 p.
17. National Research Council (NRC) [Internet]. *Guide for the Care and Use of Laboratory Animals*. Washington: National Academy of Sciences; 1996 [cited 2016 Nov 21]. Available from: <http://www.oacu.od.nih.gov/regs/guide/guide3.htm#behma>.
18. Silva MA, Merzel J. Stereological determination of the volume of the rat hemimandible tissues. *Anat Rec.* 2001;263:255-9.
19. Gundersen, HJ, Bendtsen TF, Korbo L, Marcussen N, Møller A, Nielsen K. Some new, simple and efficient stereological methods and their use in pathological research and diagnosis. *APMIS.* 1988;96:379-94.
20. Braendgaard H, Gundersen HJ. The impact of recent stereological advances on quantitative studies of the nervous system. *J Neurosci Methods.* 1986;18:39-78.
21. Nyengaard JR. Stereologic methods and their application in kidney research. *J Am Soc Nephrol.* 1999;10(5):1100-23.
22. Mandarim-de-Lacerda CA. Stereological tools in biomedical research. *An Acad Bras Cienc.* 2003;75(4):469-86.
23. Sterio DC. The unbiased estimation of number and sizes of arbitrary particles using the disector. *J Microsc.* 1984;134:127-36.
24. Thrall KD, Vucelick ME, Gies RA. Comparative metabolism of carbon tetrachloride in rats, mice, and hamsters using gas uptake and PBPK modeling. *J Toxicol Environ Health.* 2000;60:531-48.
25. Ohta Y, Kongo M, Sasaki E, Nishida K, Ishiguro I. Therapeutic effect of melatonin on carbon tetrachloride-induced acute liver injury in rats. *J Pineal Res.* 2000;28:119-26.
26. Naziroglu M, Cay M, Ustundag B, Aksakal M, Yekeler H. Protective effects of vitamin E on carbon tetrachloride-induced liver damage in rats. *Cell Biochem Funct.* 1999;17:253-9.
27. Mukai T, Mera K, Nishida K. A novel method for preparation of animal models of liver damage: liver targeting of carbon tetrachloride in rats. *Biol Pharm Bull.* 2002;25:1494-7.
28. Sanzgiri UY, Srivatsan V, Muralidhara S, Dallas CE, Bruckner JV. Uptake, distribution, and elimination of carbon tetrachloride in rat tissues following inhalation and ingestion exposures. *Toxicol Appl Pharmacol.* 1997;143:120-9.
29. Ronis M.J, Huang J, Longo V, Tindberg N, Ingelman-Sundberg M, Badger TM. Expression and distribution of cytochrome P450 enzymes in male rat kidney: Effects of ethanol, acetone and dietary conditions. *Biochem Pharmacol.* 1998;55:123-9.
30. Rush GF, Smith JH, Newton JF, Hook JB. Chemically induced nephrotoxicity: role of metabolic activation. *Crit Rev Toxicol.* 1984;13:99-160.
31. Chaiyasut C, Kusirisin W, Lailerd N, Lerttrakarnnon P, Suttajit M, Srichairatanakool S. Effects of phenolic compounds of fermented Thai indigenous plants on oxidative stress in streptozotocin-induced diabetic rats. *J Evid Based Complementary Altern Med.* 2011;2011:1-10.
32. Priyadarshini M, Atif M, Bano B. Alpha-linolenic acid protects against gentamicin induced toxicity. *Res Report Biochem.* 2012;2:25-9.
33. Ren J, Chung SH. Anti-inflammatory effect of  $\alpha$ -linolenic acid and its mode of action through the inhibition of nitric oxide production and inducible nitric oxide synthase gene expression via NF- $\kappa$ B and mitogen-activated protein kinase pathways. *J Agric Food Chem.* 2007;55:5073-80.
34. Rajeswari G, Murugan M, Mohan VR. GC-MS analysis of bioactive components of *Hugoniamystax* L. (Linaceae). *Res J Pharm Biol Chem Sci.* 2012;3:301-8.
35. Lin HM, Tseng HC, Wang CJ, Lin JJ, Lo CW, Chou FP. Hepatoprotective effects of *Solanum nigrum* Linn. extract against CCl<sub>4</sub>-induced oxidative damage in rats. *Chem Biol Interact.* 2008;171:283-93.
36. Striker GE, Smockler EA, Kohnen PW, Nagle RB. Structural and functional changes in rat kidney during CCl<sub>4</sub> intoxication. *Am J Pathol.* 1968;53:769-89.
37. Khan M.R, Zehra, H. Amelioration of CCl<sub>4</sub>-induced nephrotoxicity by *Oxalis corniculata* in rat. *Exp Toxicol Pathol.* 2013;65:327-34.
38. Khan M.R, Siddique F. Antioxidant effects of *Citharexylum spinosum* in CCl<sub>4</sub> induced nephrotoxicity in rat. *Exp Toxicol Pathol.* 2012;64:349-55.

39. Khan RA, Khan MR. Prevention of CCl<sub>4</sub>-induced nephrotoxicity with *Sonchus asper* in rat. *Food Chem Toxicol.* 2010;48:2469-76.
40. Laurinavicius A, Laurinaviciene A, Dasevicius D, Elie N, Plancoulaine B, Herlin P. Digital image analysis in pathology: Benefits and obligation. *Anal Cell Pathol.* 2012;35:75-8.
41. Pantanowitz L. Digital images and the future of digital pathology. *J Pathol Inform.* 2010;1:15.
42. Klapczynski M, Gagne GD, Morgan SJ, Larson KJ, LeRoy BE, Blomme EA, Cox BF, Shek E W. Computer-assisted imaging algorithms facilitate histomorphometric quantification of kidney damage in rodent renal failure models. *J Pathol Inform.* 2012;3:20.
43. Boyce JT, Boyce RW, Gundersen HJ. Choice of morphometric methods and consequences in the regulatory environment. *Toxicol Pathol.* 2010;38:1128-33.